DOI: 10.1002/ejic.200900972

Synthesis, Crystal Structure and Physico-Chemical Studies of Neodymium and Erbium Methoxides Containing Thienyl Substituents

Michael Veith,*[a,b] Céline Belot,[a,c] Volker Huch,[a] Hai Ling Cui,[d] Laurent Guyard,[c] Michael Knorr,[c] and Claudia Wickleder[d]

Keywords: Lanthanides / Electrochemistry / Luminescence / Thienyl methoxides

Two novel mononuclear neodymium alkoxides [Nd{OC($C_{14}H_{11}S_2$)}$_3$(thf)$_3$]·thf (**9**) and [Nd{OC($C_{16}H_{13}S$)}$_3$(thf)$_3$]·thf (**10**) have been prepared by the reaction between Nd[N($SiMe_3$)$_2$]$_3$ and the tertiary alcohols HO–C($C_{14}H_{11}S_2$) (**3**) and HO–C($C_{16}H_{13}S$) (**4**). The geometry around the neodymium metal is almost octahedral with a facial ligand arrangement similar to [Nd{OC($C_8H_5S_2$)$_3$}$_3$(thf)$_3$]·4thf (**5**), [Nd{OC(C_4H_3S)$_3$}$_3$(thf)$_3$]·thf (**7**) and Er[OC(C_4H_3S)$_3$]$_3$(thf)$_3$ (**8**) (X-ray diffraction on single crystals). The cyclic voltammograms of a series of neodymium and erbium alkoxides indicate that the electrochemical properties are essentially dominated by the organic ligands. In comparison to the carbinols HO–C($C_8H_5S_2$)$_3$ (**1**), HO–C(C_4H_3S)$_3$ (**2**), HO–C($C_{14}H_{11}S_2$) (**3**) or HO–C($C_{16}H_{13}S$) (**4**), the oxidation peak potentials of the thienyl units for the neodymium alkoxides [Nd{OC($C_8H_5S_2$)$_3$}$_3$(thf)$_3$]·4thf (**5**), [Nd{OC(C_4H_3S)$_3$}$_3$(thf)$_3$]·thf (**7**), [Nd{OC($C_{14}H_{11}S_2$)}$_3$(thf)$_3$]·thf (**9**) and [Nd{OC($C_{16}H_{13}S$)}$_3$(thf)$_3$]·thf (**10**) are marginally shifted towards higher values by 0.03–0.10 V, whereas for Er[OC($C_8H_5S_2$)$_3$]$_3$(thf) (**6**) and Er[OC(C_4H_3S)$_3$]$_3$(thf)$_3$ (**8**) a decrease of these potentials is noticed. Repetitive cyclic voltammetry does not generate polymeric films for **7**–**10**, as found for the free organic ligands **2**–**4**. Contrarily, the mononuclear precursors [Nd{OC($C_8H_5S_2$)$_3$}$_3$(thf)$_3$]·4thf (**5**) and Er[OC($C_8H_5S_2$)$_3$]$_3$(thf) (**6**) are electro-oxidized and electro-active polymer films are obtained and characterized. To investigate the positions of the excited states of the ligands, emission spectra of the carbinols **1**–**4** have been recorded. The luminescence studies of the neodymium alkoxides reveal an energy transfer from the ligand to the metal centre with a remarkable Nd emission efficiency upon ligand excitation in the case of **5**.

Introduction

During the last two decades, the photophysics of trivalent rare earth compounds have received much attention.[1–2] Indeed, these types of materials are used in many applications, for example as optical signal amplifiers,[3] lasers,[4] or as luminescence probes in biological systems and ceramic clusters.[5] Unfortunately, trivalent lanthanide ions have an intrinsic small molar absorption coefficient in the UV/Vis/NIR spectrum due to their parity-forbidden *intra*-configurational 4f–4f transitions. However, upon coordination with organic ligands acting as "antenna", leading to a transfer of absorption and transmission energy to the rare earth ion and thus increasing their luminescence efficiency, lanthanide ions coordinated by large ligands are promising candidates.[6]

Investigations on transition metal complexes containing thiophene-derived ligands have demonstrated that these compounds possess attractive physico-chemical properties and reactivities.[7–10] Indeed, compounds with electron-rich backbones are used for their high conductivities or electroluminescence.[11] In contrast, lanthanide compounds interacting with thiophene-functionalized ligands have been explored less in the past than their transition metal analogues, but are nowadays receiving more and more attention, in particular for their use as luminescent materials.[12–16] In fact, effective emission from rare earth compounds containing thienyl substituents as chromophores has been recently reported. These thiophene derivatives are promising candidates as sensitizers.[14a,17–20]

Our own efforts have focused on the synthesis of novel lanthanide compounds containing ligands with thiophene substituents,[21] which are electrochemically active and can even be electropolymerized in some cases.[22] Moreover, the compounds presented in this paper are assumed to be very efficient as luminescent materials due to the lack of groups like OH or NH in the ligand sphere, which usually lead to quenching processes in the case of lanthanide ions emitting in the NIR range.[1a,23–26]

[a] Institute for Inorganic Chemistry, Saarland University, Campus C4 1, 66123 Saarbrücken, Germany
[b] INM – Leibniz Institute for New Materials, Campus D2 2, 66123 Saarbrücken, Germany
Fax: +49-681-9300 223
E-mail: michael.veith@inm-gmbh.de
[c] Institut UTINAM UMR CNRS 6213, Université de Franche-Comté, 16, Route de Gray, 25030 Besançon, France
[d] Inorganic Chemistry II, University of Siegen, Adolf-Reichwein-Straße, 57068 Siegen, Germany
Supporting information for this article is available on the WWW under http://dx.doi.org/10.1002/ejic.200900972.

In a previous paper,[21] we have presented the syntheses and crystal structures of a series of rare-earth methoxides of Nd^{III} and Er^{III} functionalized with thienyl substituents. We now add the syntheses of two new neodymium alkoxides, their structural characterisation and report on the electrochemical and photoluminescence properties of a whole series of Nd and Er compounds.

Results and Discussions

The lanthanide alkoxides **5**–**8** were synthesized by following the procedure described previously by the reaction between $M[N(SiMe_3)_2]_3$ ($M = Nd^{3+}$, Er^{3+}) and the thiophenic tertiary alcohols $HO–C(C_8H_5S_2)_3$ (**1**) or $HO–C(C_4H_3S)_3$ (**2**) according to Scheme 1.[21]

In this article two new derivatives of neodymium are presented. In comparison to **5** to **8** they have less thienyl and more phenyl substituents.

$[Nd\{OC(C_{14}H_{11}S_2)\}_3(thf)_3]\cdot thf$ (**9**) and $[Nd\{OC(C_{16}H_{13}S)\}_3(thf)_3]\cdot thf$ (**10**) were synthesized by reacting three equivalents of the carbinols and one equivalent of silyl amide $[Nd\{N(SiMe_3)_2\}_3]$ in tetrahydrofuran for two days at room temperature (Scheme 2). After concentration of the solutions, blue air-sensitive single-crystals of **9** and **10** were obtained in 60 and 34% yield, respectively. Despite this coloration, which is most probably due to the weak f–f transitions of the neodymium metal centres, the UV/Vis spectra display only strong absorptions at 237 and 232 nm, respectively, attributed to the $\pi\rightarrow\pi^*$ transitions of the aromatic groups.

The ^{1}H-NMR spectrum of **9** recorded in $CDCl_3$ exhibits only broad peaks, probably due to the paramagnetic character of the neodymium metal centre. The broad signal at 7.3 ppm, which integrates for 21 H, is attributed to the fifteen hydrogen atoms of the phenyl groups and the six 5-H of the thienyl units. Another aromatic signal, at 6.9 ppm, integrating for 12 H, corresponds to 4-H and 3-H of the thienyl groups. The spectrum displays four other broad signals at 3.7, 1.8, 1.2 and 0.8 ppm due to the different hydrogen atoms of the tetrahydrofuran molecules, with or without bonding to neodymium. As noticed for the other neodymium alkoxides (**5**, **7** and **9**),[21] the ^{1}H-NMR spectrum of **10** displays broad signals at room temperature in $CDCl_3$. Three aromatic signals are present at 7.3, 6.9 and 6.7 ppm. The first one, which integrates for 33 H, corresponds to the three 5-H of the thienyl units and to the thirty protons of the six phenyl groups. The second and the third ones, integrating each for 3 H, are attributed to the 4-H and 3-H of the thienyl groups, respectively. The remaining other signals at 3.6, 1.7, 1.2 and 0.8 ppm are assigned to the different hydrogen atoms of the tetrahydrofuran molecules ligated or not to the metal centre.

X-ray Structure Determinations of the Rare Earth Thienyl-Substituted Methoxides

According to the X-ray diffraction studies presented in our previous paper,[21] the coordination spheres around the metal centres are approximately octahedral for $[Nd\{OC(C_8H_5S_2)_3\}_3(thf)_3]\cdot 4thf$ (**5**), $[Nd\{OC(C_4H_3S)_3\}_3(thf)_3]\cdot thf$ (**7**) and $Er[OC(C_4H_3S)_3]_3(thf)_3$ (**8**), whereas a tetrahedral geometry around the erbium ion was established

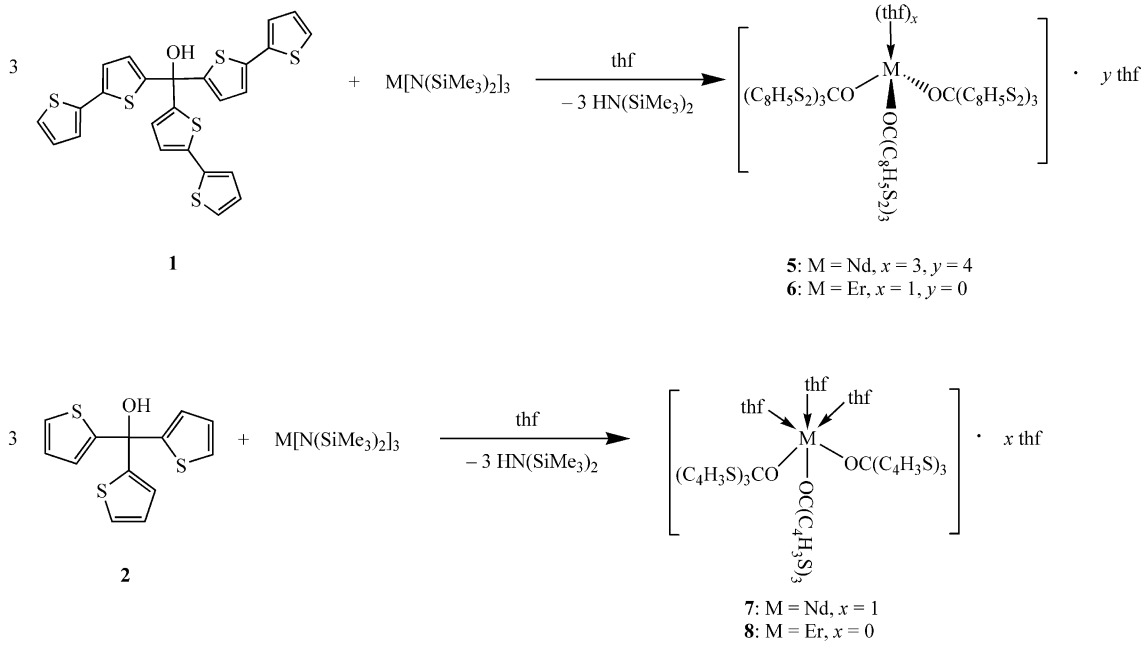

Scheme 1. Synthesis of the rare earth thienyl methoxides **5**–**8**.

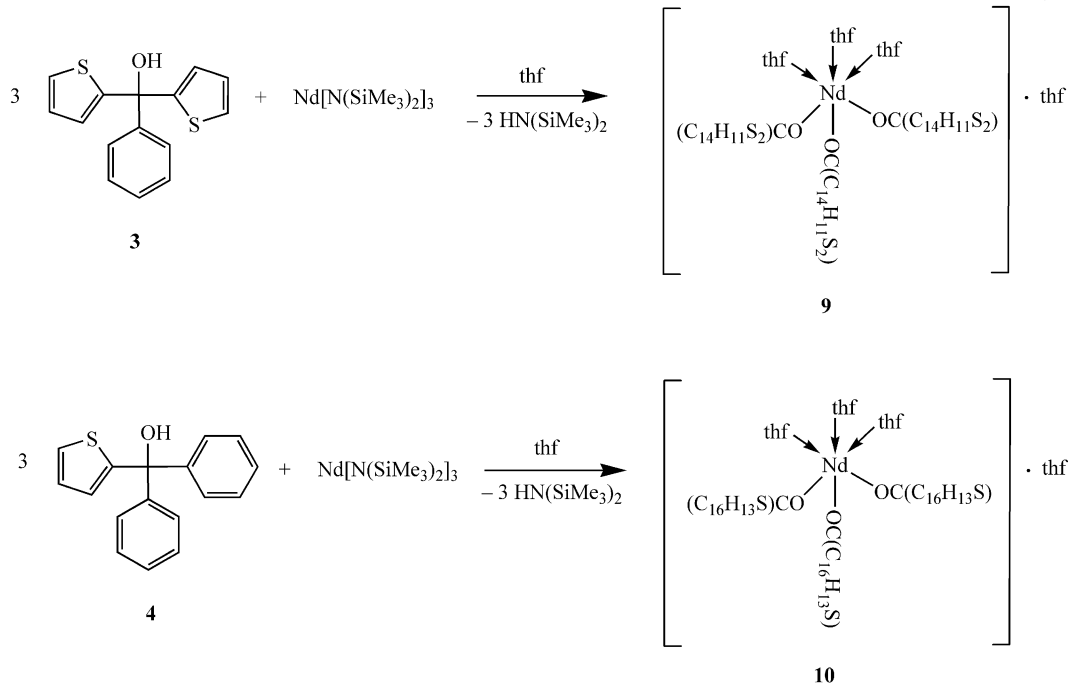

Scheme 2. Synthesis of the neodymium thienyl-substituted methoxides **9** and **10**.

for $Er[OC(C_8H_5S_2)_3]_3(thf)$ (**6**). Single-crystal X-ray structure determinations were also performed for compounds **9** and **10**, which both crystallize at 5 °C from tetrahydrofuran as blue crystals. Selected bond lengths and angles are summarized in Table 1. Unfortunately, for **10** the differentiation between the thienyl and phenyl groups is difficult. This may be attributed to the fact that the crystallization process has taken place with a disordered arrangement of the thienyl and phenyl groups.

Table 1. Selected bond lengths [Å] and angles [°] for **9** and **10**.

	9	**10**
Nd–O(1)	2.184(4)	2.178(4)
Nd–O(2)	2.635(4)	2.595(6)
O(1)–C(1)	1.388(6)	1.397(7)
O(1)–Nd–O(1)	100.0(2)	102.1(2)
O(1)–Nd–O(2)	93.2(2)	90.4(2)
O(2)–Nd–O(2)	73.6(2)	76.9(2)
C(1)–O(1)–Nd	168.9(4)	173.9(4)

The structure determinations of **9** and **10** confirm the formation of mononuclear compounds with an approximately octahedral geometry around the neodymium atoms. The metal centres are surrounded by three phenylbis(2-thienyl)methoxido or diphenyl(2-thienyl)methoxido ligands and three tetrahydrofuran molecules in a facial arrangement (Figure 1). The molecules are situated on threefold axes in the crystals. Additional thf molecules are in the lattice with no interaction with the central molecules. The overall structures are similar to that of $[Nd\{OC(C_8H_5S_2)_3\}_3(thf)_3]\cdot 4thf$ (**5**), $[Nd\{OC(C_4H_3S)_3\}_3(thf)_3]\cdot thf$ (**7**),[21] $Sm(O\text{-}2,6\text{-}iPr_2C_6H_3)_3(thf)_3$[27] and $Sm(O2,4,6\text{-}Me_3C_6H_2)_3(thf)_3$.[28] The Nd–$OC(C_{14}H_{11}S_2)$ and Nd–$OC(C_{16}H_{13}S)$ distances are in the range of 2.184(4) Å (**9**) and 2.178(4) Å (**10**) comparable to those obtained for $[Nd\{OC(C_8H_5S_2)_3\}_3(thf)_3]\cdot 4thf$ (**5**) [2.193(5) Å], $[Nd\{OC(C_4H_3S)_3\}_3(thf)_3]\cdot thf$ (**7**) [2.186(1) Å],[21] $Nd(OCtBu_2CH_2PMe_2)_3$ [2.174(2) Å],[29] or for the five-coordinated neodymium in $Nd(tritox)_3(CH_3CN)_2$ [2.149(5)–2.171(5) Å].[30] The Nd–O(thf) distances range from 2.635(4) Å (**9**) to 2.595 Å (**10**) and compare with those found for $[Nd\{OC(C_4H_3S)_3\}_3(thf)_3]\cdot thf$ (**7**) [2.620(2) Å][21] or $[Nd_3(\mu_3\text{-}OtBu)_2(\mu_2\text{-}OtBu)_3(OtBu)_4(thf)_2]$ [2.661(4) Å].[31] The O–Nd–O bond angles for **9** and **10** are in the range of those observed for $[Nd\{OC(C_4H_3S)_3\}_3(thf)_3]\cdot thf$ (**7**).[21] Nevertheless, some variations of angles compared to those in $[Nd\{OC(C_8H_5S_2)_3\}_3(thf)_3]\cdot 4thf$ (**5**)[21] can be rationalized by the weaker steric repulsion exerted by the ligands in **9** and **10**.

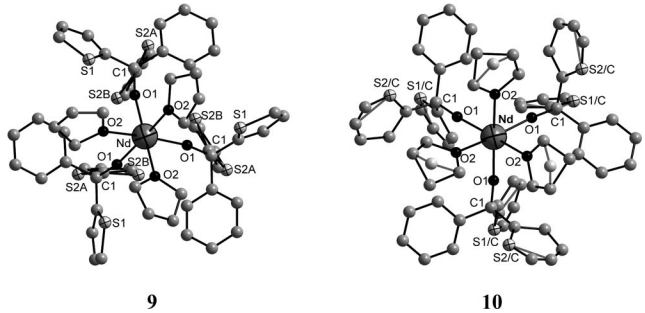

Figure 1. Molecular structures of $[Nd\{OC(C_{14}H_{11}S_2)\}_3(thf)_3]\cdot thf$ (**9**) and $[Nd\{OC(C_{16}H_{13}S)\}_3(thf)_3]\cdot thf$ (**10**). Thf lattice molecules and hydrogen atoms are omitted for more clarity. For **9**, the sulfur atoms S(2) are found in two split-positions [S(2A) and S(2B)]. For **10**, the thienyl and phenyl units are found in different positions [S(1) and S(2)] as well as the carbon atoms of the thf.

In conclusion, these structural studies demonstrate that a variation of the number of thienyl groups of the methoxides does not affect the nuclearity and geometry around the neodymium metal centre. Only some minor variations of the bond lengths are noticed, whereas the angle values are somewhat more affected due to the different steric bulk of the ligands.

Electrochemical Studies

Nowadays, the electropolymerization of thiophene and its derivatives is a well-established routine technique to generate polymeric films on the surface of electrodes or semiconducting surfaces.[32–33] Since the last decade, the incorporation of transition metal centres into the polythiophene film has emerged as interesting extensions, thus combining the intrinsic properties of transition metal ions with those of polythiophenes. One method to achieve the generation of metal-containing polymers consists in the elaboration of thiophene-functionalized ligands, which are subsequently coordinated to a transition metal and are finally electropolymerized in the last step. For example, Beley et al. coordinated thiophene-functionalized terpyridines on Ru^{II}. The electropolymerization of the resulting chelate complexes lead to the generation of an electroactive layer, which could be deposited on the electrodes.[10] The groups of Wolf et al. and Constable et al. demonstrated in a series of papers the possibility to electropolymerize thiophene-functionalized complexes of Os^{II}, Pd^{II} and Au^{I}.[7–8,34] Others used more simple model compounds to study the influence of the metal on the oxidation process. For example, Lin et al. have synthesized some ferrocenyl-Pd/Pt complexes with thiophene spacers. They found that oxidation of theses complexes leads to a voltammogram where the wave of ferrocene is shifted to negative values. This shift is due to a delocalization of electrons from the metal on ferrocene over the spacer.[35] The influence of a metal on the position of the oxidation waves of metal-containing polymers was also addressed.[7–8,36–37]

In contrast, the electropolymerization of suitable lanthanide complexes is barely documented.[12] Therefore, it appeared tempting to probe whether our thiophene-functionalized complexes **5**–**10** are electrochemically active and may be used as precursors for electropolymerization studies. To evaluate the influence of the lanthanide(III) ion on the targeted polymeric materials, we used both spectroscopy and electrochemistry as tools. Unfortunately, the interpretation of the results obtained with these two techniques was not trivial to rationalize (spectral broadening, additional electrochemical peaks).

The values of the peak potentials for the organic ligands **1**, **2**, **3** and **4** and its derived rare earth alkoxides **5**–**10** are given in Table 2.

Organic Ligands 1–4

The cyclic voltammogram of **1** at 100 $mV\,s^{-1}$ (or at 500 $mV\,s^{-1}$) shows two oxidation waves at 0.92 and 1.68 V (or 0.97 and 2.02 V) (Figure 2, a). The first peak potential is attributed to the oxidation of the dithienyl units forming the radical cation;[38] the second could be assigned to the oxidation of the radical cation leading to a dication[39a–39b] and/or to the oxidation of the oligomers formed during the polymerization process. The intensity of the first oxidation peak appears very weak compared to the second one. This phenomenon has been already observed for the compound 5,5′-bis([2.2]paracyclophanyl)-2,2′-bithiophene.[39b] In our case, the high intensity and the shape of the second oxidation wave seem to indicate an adsorption process on the working electrode.[39c] The reduction wave at 0.38 V (or 0.56 V) corresponds to the reduction of the dication and/or of the oligomers and this at –0.25 V (or –0.39 V) to the reduction of the carbocation. Indeed, during the oxidation process, some H^+ are liberated and can react with the carbinol to form a stable carbocation (Scheme 3).[22] The electrochemical studies of **1** are in agreement with those obtained in previous experiments.[22,40]

The oxidation of **2** between –0.50 and +2.00 V on a platinum electrode at 100 $mV\,s^{-1}$ leads to an irreversible wave (Figure 2, b) at 1.48 V. This peak is assigned to the oxidation of the thienyl units and the value is in agreement with other compounds containing thienyl units (for exam-

Table 2. Values of standard potentials or compounds **1**–**10** in dichloromethane (vs. $Ag/AgClO_4$) deduced from cyclic voltammetric measurements.

Compounds	100 $mV\,s^{-1}$		500 $mV\,s^{-1}$	
	E_{pa} [V]	E_{pc} [V]	E_{pa} [V]	E_{pc} [V]
$HO–C(C_8H_5S_2)_3$ (**1**)	0.92[a], 1.68[b]	0.38[c], –0.25[d]	0.97[a], 2.02[b]	0.56[c], –0.39[d]
$[Nd\{OC(C_8H_5S_2)_3\}_3(thf)_3]\cdot 4thf$ (**5**)	0.95[a], 1.41[b]	0.95[c], –0.42[d]	1.13[a], 1.55[b]	0.89[c], –0.46[d]
$Er[OC(C_8H_5S_2)_3]_3(thf)$ (**6**)	0.81[a], 1.19[b]	0.64[c], –0.66[d]	0.79[a], 1.22[b]	0.66[c], –0.64[d]
$HO–C(C_4H_3S)_3$ (**2**)	1.48[a]	–0.20[d]	1.50[a]	–0.21[d]
$[Nd\{OC(C_4H_3S)_3\}_3(thf)_3]\cdot thf$ (**7**)	1.53[a]	–	1.59[a]	–0.27[d]
$Er[OC(C_4H_3S)_3]_3(thf)_3$ (**8**)	1.39[a]	–0.32[d]	1.44[a]	–0.37[d]
$HO–C(C_{14}H_{11}S_2)$ (**3**)	1.43[a]	–0.19[d]	1.66[a]	–0.22[d]
$[Nd\{OC(C_{14}H_{11}S_2)\}_3(thf)_3]\cdot thf$ (**9**)	1.53[a]	–0.19[d]	1.77[a]	–0.26[d]
$HO–C(C_{16}H_{13}S)$ (**4**)	1.64[a]	–0.22[d]	1.72[a]	–0.17[d]
$[Nd\{OC(C_{16}H_{13}S)\}_3(thf)_3]\cdot thf$ (**10**)	1.66[a]	–0.10[d]	1.79[a]	–0.21[d]

[a] Oxidation of the thienyl units forming the cation radical. [b] Oxidation of the radical cation leading to a dication and/or oxidation of the oligomers. [c] Reduction of the dication and/or of the oligomers. [d] Reduction of the carbocation.

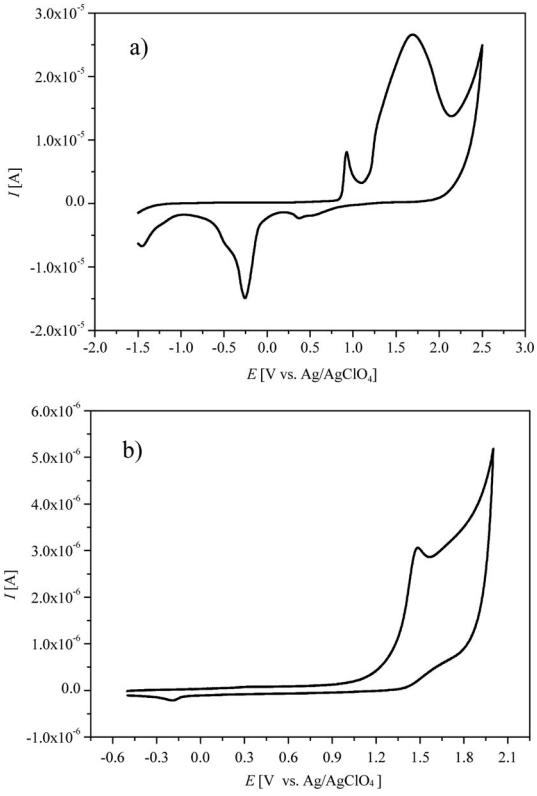

Figure 2. Representative cyclic voltammograms recorded on a platinum electrode in a dichloromethane solution containing a) **1** (10^{-3} M) b) **2** (10^{-3} M) and $[NBu_4][PF_6]$ (0.1 M), vs. $Ag/AgClO_4$, scan rate 100 mV s^{-1}.

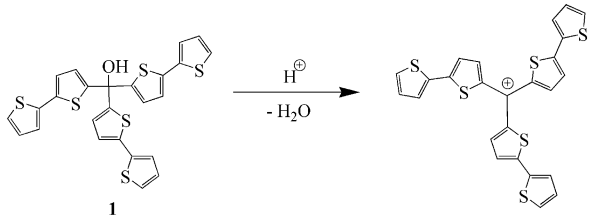

1

Scheme 3. Formation of carbocation by protonation and water abstraction from $HO–C(C_8H_5S_2)_3$ (**1**).

ple 3,4-propylenedisulfanylthiophene).[41] A second wave is observed on the cyclic voltammogram at –0.20 V and corresponds to the reduction of the carbocation generated during the process. By repetitive oxidation of a solution of **2**, no formation of a polymeric film was observed. This finding may be explained by the difficulty in generating a stable radical cation with thiophene units.[42–45]

The behaviour of **3** or **4** towards oxidation is similar to what is observed for **2**. The oxidation peak is located at 1.48 V for **2**, 1.43 V for **3** and 1.64 V for **4** at 100 mV s^{-1}. The introduction of phenyl group(s) instead of thienyl group(s) does not lead to a significant variation of the oxidation values. Therefore, it can be concluded that the electronic effects of the phenyl or thienyl groups in the electrochemical behaviour of these types of compounds are quite similar. Nevertheless, compared with **1**, the oxidation peak potentials of **2**–**4** are shifted towards higher values. Indeed, generally, extending the length of a π-system results in a decrease in the oxidation potential.[7b,46]

Rare Earth Alkoxides 5–10

Neodymium Alkoxides

The cyclic voltammogram of **5** at 100 mV s^{-1} exhibits oxidation waves assigned to the bithienyl units and two reduction waves are measured which are attributed to the reduction of the dication or to the reduction of the oligomers and to the reduction of the carbocation (see below). The same observations have been made at 500 mV s^{-1}. No oxidation or reduction waves due to the metal centre have been observed. The oxidation peak of **5** is shifted towards higher potentials, compared to the oxidation peak of **1**. There are two factors which may contribute to this shift: the inductive effect of the metal and the change in the interannular conjugation within the structure of the metal alkoxide.[7b]

When the potential is cycled with compound **5**, at 500 mV s^{-1} for example, the deposition of a material on the electrode is observed (Figure 3, a) via the coupling of the α-position of the terminal dithienyl rings.[7c] From the second cycle, a new oxidation wave at 0.40 V is present due to the oxidation of an unknown product formed during the cycling. The resulting thin film obtained after five cycles is characterized by an electrochemical experiment in a solution containing only the solvent and the supporting electrolyte, without monomers. It displays an electroactive character analogous to polythiophene,[38,47] with a broad reversible peak at an average potential of 1.23 V and a reduction wave at –0.70 V assigned to the carbocation (Figure 3, b). The presence of the carbocation indicates a de-coordination of the neodymium alkoxide. However, no further proofs confirming a metal deposition in the polymer film can be added at this time. Nevertheless, when comparing the intensity of the oxidation wave of **5** and the intensity of the reduction wave of the carbocation, we can conclude that only a small part of the metal is eliminated. The curves shown in Figure 3 (parts a and b) are characteristic of the formation of electroactive polythiophene polymers.[22,38,48] Note that an oxidation wave at 0.13 V is observed corresponding to an unidentified species formed during the deposition.

The cyclic voltammograms of **7**, **9** and **10**, at 100 mV s^{-1}, lead again only to an irreversible peak due to the oxidation of the organic ligands and a reduction wave due to the reduction of the carbocation (excepted for **7**: the lifetime of this species is not long enough to be reduced during the experiment at this scan rate). No polymeric film is obtained during the cycling in accordance with their corresponding carbinols.

The oxidation values of the metal derivatives are marginally increased in comparison with the carbinols **1**–**4** (by 0.03–0.10 V, see Table 2). We can conclude that a weak electronic transfer inside the molecule exists.[7b,10] In our case,

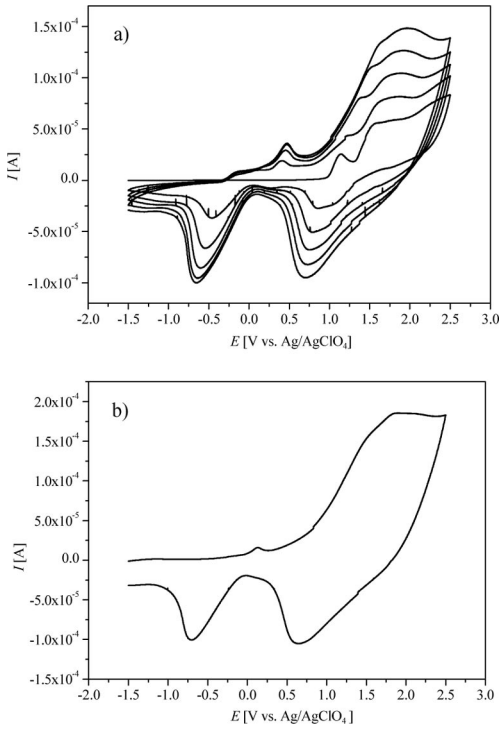

Figure 3. a) Repetitive cyclic voltammetry recorded on a platinum electrode in a dichloromethane solution containing **5** (10^{-3} M) and $[NBu_4][PF_6]$ (0.1 M), vs. $Ag/AgClO_4$, scan rate 500 mV s^{-1}; b) cyclic voltammogram of polymeric **5**, prepared by five oxidation–reduction cycles on a platinum electrode at 500 mV s^{-1}, in dichloromethane $[NBu_4][PF_6]$ (0.1 M), vs. $Ag/AgClO_4$, scan rate 500 mV s^{-1}.

the electron-rich groups have a donor-effect on the neodymium leading to a more difficult oxidation process of the dithienyl or thienyl heterocycles.

Erbium Alkoxides

The cyclic voltammogram of erbium compound **6** displays at 500 mV s^{-1} (or at 100 mV s^{-1}) two oxidation waves at 0.79 and 1.22 V (or 0.81 and 1.19 V) corresponding to the oxidations of the dithienyl units, as well as two reduction waves at 0.66 and –0.64 V (or 0.64 and –0.66 V) due to the reduction of the dication and/or of the oligomers and the carbocation, respectively. No oxidation or reduction waves at the metal centre have been obtained. Contrarily to the neodymium alkoxide **5**, the oxidation peak is shifted to lower values in comparison with compound **1**. When the potential is cycled at 100 or 500 mV s^{-1}, a polymeric film on the platinum electrode is deposited (see Supporting Information). From the second cycle, a new oxidation wave (–0.41 V at 500 mV s^{-1}) is present due to the oxidation of an unknown product formed during the cycling. The resulting thin film obtained after four cycles at 500 mV s^{-1} is characterized by an electrochemical experiment in a solution containing only the solvent and the supporting electrolyte, without monomers. It displays, as its neodymium analogue (see above), an electroactive character with a broad reversible peak at an average potential of 1.02 V and a reduction wave at –0.64 V assigned to the carbocation (see Supporting Information). As mentioned above for **5**, the observed carbocation implies again a decoordination of the erbium alkoxide. Moreover, an oxidation wave at –0.12 V is observed corresponding to an unidentified species formed during the deposition.

The cyclic voltammogram of the erbium compound **8** at 100 mV s^{-1} (or at 500 mV s^{-1}) shows an irreversible oxidation wave at 1.39 V (or 1.44 V) attributed to the oxidation of the thienyl and a reduction peak at –0.32 V (or –0.37 V) due to reduction of the carbocation.

By comparison with the carbinols **1** and **2** and contrarily to the results obtained for the neodymium alkoxides, the oxidation values of the bithienyl (**6**) or thienyl (**8**) units are shifted towards lower values (0.14 and 0.09 V, respectively). Again, an electronic transfer inside the molecules is present. But here, the erbium metal centres have a donor-effect giving rise to an easier heterocycle oxidation process which translates as a decrease of the oxidation potentials.

Luminescence Studies

Recently, several studies have demonstrated that thiophene-derived ligand systems can be promising candidates for sensitizer chromophore in lanthanide compounds.[17–20] In these examples, the complexes possess a conjugation between the donor (the ligand) and the acceptor (the lanthanide ion). But in our case, the conjugation is interrupted by the methoxido group and no interaction via π-conjugation between the thiophene units and the lanthanides are present (spatial distance from the aromatic groups to the metal: ca. 5 Å). Therefore, it was intriguing to study, if, in these conditions, an antenna effect is possible or not.

All luminescence spectra were recorded in the solid state to limit the dissociation of the compounds during the measurements. Nevertheless, the investigations of $Er[OC(C_8H_5S_2)_3]_3(thf)$ (**6**) and $Er[OC(C_4H_3S)_3]_3(thf)_3$ (**8**) could not be performed due to a photodegradation during the experiments, indicated by a colour change of the erbium alkoxides.

Carbinols

First the carbinols were investigated to get more information about the ability of the methoxido ligands to act as chromophore and about the position of the electronic excited states.

The luminescence spectra of the compounds $HO–C(C_8H_5S_2)_3$ (**1**) and $HO–C(C_4H_3S)_3$ (**2**) are depicted in Figures 4 and 5. Both compounds show broad emission bands which can be assigned to $\pi^* \rightarrow \pi$ transitions of the thienyl units. The maxima are located at about 488 and 538 nm (**1**) as well as at 430 nm (**2**), respectively. As expected, the red shift of the maxima of **1** compared to those of **2** is due to the increased size of the π-system in the latter.[49] Excitation spectra are also shown in Figures 4 and 5. The excitation spectrum of **2** has a maximum at 356 nm, while for compound **1** two maxima at about 423 and 464 nm were found with emission detection at energies of the two emission bands. This clearly shows that these emission bands do not

belong to one thiophenic unit, but must be assigned to two units with different conformations with regard to one another.

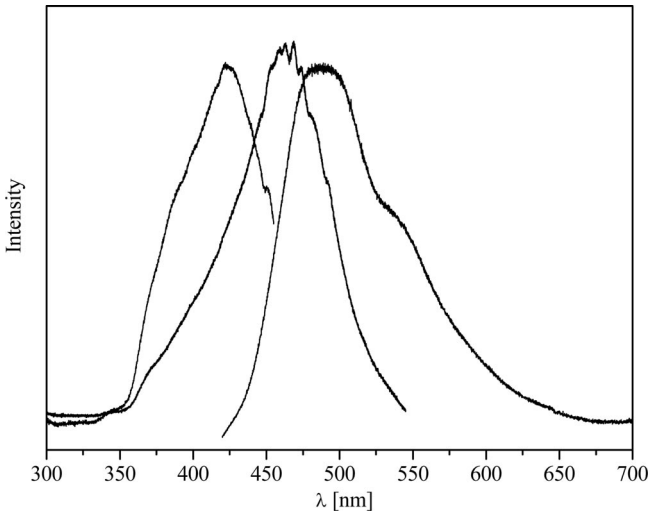

Figure 4. Room temperature solid-state luminescence spectra HO–$C(C_8H_5S_2)_3$ (**1**). Left: excitation spectrum, λ_{em} = 470 nm; Centre: excitation spectrum, λ_{em} = 560 nm. Right: emission spectrum, λ_{ex} = 400 nm.

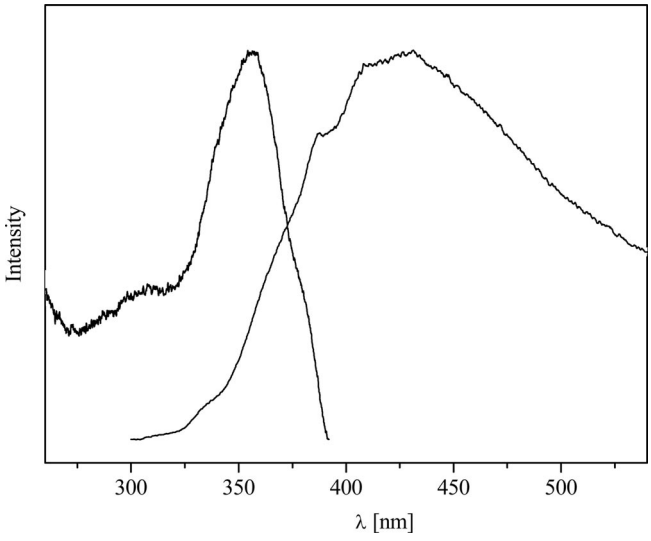

Figure 5. Room temperature solid-state luminescence spectra of HO–$C(C_4H_3S)_3$ (**2**). Left: excitation spectrum, λ_{em} = 410 nm. Right: emission spectrum, λ_{ex} = 280 nm.

The luminescence behaviour of **3** or **4** is quite similar to what is observed for **2** ($\pi^*\rightarrow\pi$ transitions of the thienyl and phenyl units). The emission maxima are located at 430 nm for **2**, 402 nm for **3** and 392 for **4**: the introduction of phenyl group(s) instead of thienyl group(s) leads to a blue shift of these emission bands.

Neodymium Alkoxides

Room temperature emission spectra of $[Nd\{OC(C_8H_5S_2)_3\}_3(thf)_3]\cdot 4thf$ (**5**) and $[Nd\{OC(C_4H_3S)_3\}_3(thf)_3]\cdot$ thf (**7**) in the NIR range upon excitation of the ligands (see below) are depicted in Figure 6. Typical Nd^{3+} $4f^3\rightarrow 4f^3$ transitions are detected which can be assigned to emission from the excited $^4F_{3/2}$ state to $^4I_{9/2}$ (around 900 nm), $^4I_{11/2}$ (1070 nm), and $^4I_{13/2}$ (1350 nm) ground states (the same observations have been made for **9** and **10**, see Supporting Information).[50–52] Compared to the pure inorganic Nd compounds, the bands are relatively broad and no crystal field splitting is resolved. The clear spectrum is typical for an "antenna effect", resulting in an energy transfer from the ligand to the lanthanide centre.[53] No ligand emission bands could be detected in the visible region of the spectrum leading to the assumption of relatively efficient energy transfer processes.

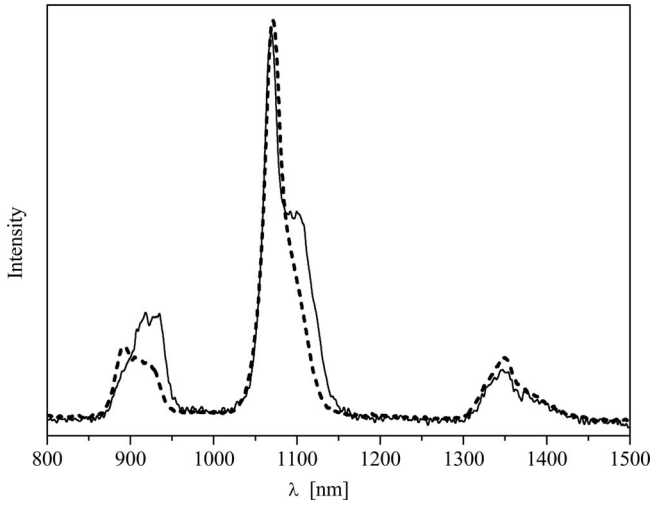

Figure 6. NIR solid-state emission spectra at room temperature for compounds **5** (dotted line) and **7** (solid line), λ_{ex} = 373 (**5**) and 347 nm (**7**).

The respective excitation spectra monitoring the $^4F_{3/2}\rightarrow{}^4I_{11/2}$ transition (Figure 7) consist of bands corresponding to Nd^{3+} f–f transitions, as well as broader bands due to the ligand transitions (the same observations have been made for **9** and **10**, see Supporting Information). The maxima and assignments of the compound **7** are listed in Table 3. Due to the multiplicity of excited 4f states in the visible region, some transitions to different states are not resolved and, again, the bands are relatively broad compared to doped compounds.[54] The ligand bands are located at 373 nm (**5**) and 345 nm (**7**), respectively. Due to the larger π-system, the maximum for **5** is at lower energy.[49] For **9** a similar value as for **5** (375 nm) is found whereas **10** has a maximum at 360 nm (see Supporting Information).

The energy transfer from the ligand to Nd is proven by the presence of ligand excitation bands while monitoring the Nd emission. Moreover, the differences of the relative intensities of the ligand and Nd excitation bands give further information about the energy transfer efficiency. For **7** (or **9** or **10** see Supporting Information), the intensity of the Nd 4f bands is much higher than those of the ligand bands. Therefore, Nd emission intensity is more important if exciting Nd directly than exciting the ligands, especially

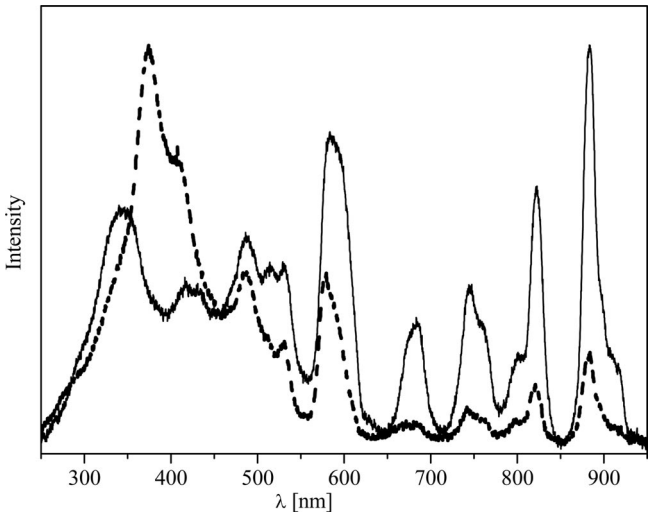

Figure 7. Solid-state excitation spectra at room temperature for compounds **5** (dashed line) and **7** (solid line), λ_{em} = 1070 nm.

Table 3. Maxima and assignments of Nd^{3+} f–f transitions of **7**.

Transitions	Wavelengths [nm]
$^4I_{9/2} \rightarrow {}^4F_{3/2}$	884
$^4I_{9/2} \rightarrow {}^4F_{5/2}$	822
$^4I_{9/2} \rightarrow {}^4F_{7/2}$	746
$^4I_{9/2} \rightarrow {}^4F_{9/2}$	682
$^4I_{9/2} \rightarrow {}^4G_{5/2}/{}^2G_{7/2}$	585
$^4I_{9/2} \rightarrow {}^4G_{7/2-9/2}/{}^2K_{13/2}$	530, 512
$^4I_{9/2} \rightarrow {}^4G_{9/2}/{}^2K_{15/2}$	486
$^4I_{9/2} \rightarrow {}^4G_{11/2}/{}^2P_{1/2}$	420

because 4f–4f transitions are forbidden and, thus, rather weak. On the other hand, the absence of ligand emission shows that the energy transfer is not inefficient or the ligand emission is fully quenched. As the latter is not very probable, the Nd emission may be rather quenched by some amount after ligand excitation, but not after Nd excitation. The situation is different in the case of **5**, where the excitation ratio I(ligands)/I(Nd) is much higher, showing a much more efficient Nd emission after ligand excitation. The reason for this is not known, and we are not able to investigate the mechanism due to the lack of equipment to measure lifetimes in the NIR range. The mechanism is, however, most probably of the Förster type due to the large spatial distances between the ligands and the Nd ions which are in the range of 5 Å.[55] In general, the observation of Nd NIR emission bands after ligand excitation shows the applicability for the present ligands in this context due to the lack of high-energy phonons.[56]

Conclusions and Perspectives

The reaction between the carbinol diphenyl(2-thienyl)-methanol (**3**) or phenylbis(2-thienyl)methanol (**4**) and the neodymium silyl amide yields the mononuclear alkoxides $[Nd\{OC(C_{14}H_{11}S_2)\}_3(thf)_3]\cdot thf$ (**9**) and $[Nd\{OC(C_{16}H_{13}S)\}_3(thf)_3]\cdot thf$ (**10**), respectively. We have shown that the geometry around the neodymium metal centre is almost octahedral with a facial ligand arrangement in accordance with $[Nd\{OC(C_8H_5S_2)_3\}_3(thf)_3]\cdot 4thf$ (**5**) and $[Nd\{OC(C_4H_3S)_3\}_3(thf)_3]\cdot thf$ (**7**).

The physico-chemical investigations of the series of neodymium or erbium methoxides containing thienyl substituents have shown that the electrochemical properties are above all dominated by the organic ligands. The repetitive cyclic voltammetry of $[Nd\{OC(C_8H_5S_2)_3\}_3(thf)_3]\cdot 4thf$ (**5**) and $Er[OC(C_8H_5S_2)_3]_3(thf)$ (**6**) leads to the formation of polymeric films which have an electroactive character. The oxidation values of the thienyl units are marginally increased for the neodymium alkoxides or decreased for the erbium alkoxides, in comparison with their corresponding carbinols: therefore, from an electrochemical point of view, the electronic transfers from metal to ligands or from ligands to metal are weak. Nevertheless, the luminescence spectra of the Nd^{3+} alkoxides exhibit an energy transfer from the ligand to the lanthanide centre. The more extended π ligand system of **5** leads to a considerably more intense Nd emission.

The examination of the physico-chemical properties of the polymeric films obtained and their characterization by AFM microscopy and other techniques are in progress. Furthermore, an extension on the reactivity of these carbinols towards other lanthanides (Eu^{3+}, Tb^{3+}, Sm^{3+}) is underway.

Experimental Section

General: All reactions were performed under nitrogen atmosphere in a Schlenk apparatus. The solvents (thf, diethyl ether, toluene and benzene) were distilled from sodium and kept under nitrogen. Dichloromethane was distilled from $CaCl_2$ and kept under nitrogen. $Nd[N(SiMe_3)_2]_3$ and $Er[N(SiMe_3)_2]_3$,[57] tris(2,2′-bithienyl-5-yl)methanol (**1**),[58] tris(2-thienyl)methanol (**2**), phenylbis(2-thienyl)-methanol (**3**) and diphenyl(2-thienyl)methanol (**4**)[59] were prepared according to the literature. The ^1H NMR spectra were recorded on a Bruker ACF-NMR (200 MHz) or a Bruker Avance 400 spectrometer (400 MHz, H,H-COSY). The UV/Vis spectra were obtained on a Perkin–Elmer Lambda 35 spectrometer. Analytical data were measured with a LECO CHN-900 instrument.

Cyclic voltammetric experiments were performed at room temperature on an Autolab PGSTAT 20 Potentiostat Galvanostat (Ecochemie) equipped with a three-electrode assembly with 0.1 M $[NBu_4][PF_6]$ (TBAF) as supporting electrolyte and CH_2Cl_2 as solvent. The working electrode was a platinum disk of 1 mm in diameter. It was polished consecutively with polishing alumina and diamond suspension between the runs. The reference electrode was $Ag/AgClO_4$ (0.1 M in CH_3CN). A platinum disk was used as an auxiliary electrode. The solvent was freshly distilled and the solutions were prepared under nitrogen atmosphere and purged with N_2 before the first scan. The scan rates employed were 100 and 500 mV s^{-1}. The concentration of the monomeric substrates was approximately 10^{-3} M. Under these conditions, the $E_{1/2}$ of $Cp_2Fe^{+/0}$ was found to be 0.16 V (CH_2Cl_2) vs. an $Ag/AgClO_4$ reference.

Solid-state emission and excitation spectra were recorded at room temperature on a Jobin–Yvon Fluorolog-3 spectrometer equipped with a 1000 W Xenon lamp, two double grated monochromators

Table 4. X-ray crystallographic and refinement data for **9** and **10**.

Compounds	$[Nd\{OC(C_{14}H_{11}S_2)\}_3(thf)_3]\cdot thf$ (**9**)	$[Nd\{OC(C_{16}H_{13}S)\}_3(thf)_3]\cdot thf$ (**10**)
Empirical formula	$C_{61}H_{65}NdO_7S_6$	$C_{67}H_{71}NdO_7S_3$
Formula weight	1246.73	1228.66
Temperature [K]	180(2)	150(2)
Crystal system	rhombohedral	trigonal
Space group	*R*3	*P*31*c*
a [Å]	14.135(1)	14.602(1)
b [Å]	14.135(1)	14.602(1)
c [Å]	24.897(2)	15.893(1)
α [°]	90	90
β [°]	90	90
γ [°]	120	120
Volume [Å^3]	4307.8(3)	2934.9(3)
Z	3	2
ρ_{calc} [mg/m^3]	1.442	1.390
μ [mm^{-1}]	1.174	1.045
F(000)	1929	1274
Crystal size [mm^3]	0.44 × 0.3 × 0.25	0.31 × 0.28 × 0.18
Theta range for data collection [°]	1.85 to 28.31	1.61 to 27.18
Reflexion collected	33002	59099
Independent reflections	4775 [*R*(int) = 0.0378]	4365 [*R*(int) = 0.0546]
Completeness to θ = 28.31° (**9**) and 27.18° (**10**) [%]	99.9	100.0
Absorption correction	multiscan	multiscan
Data / restraints / parameters	4775 / 9 / 210	4365 / 1 / 174
Goodness-of-fit on F^2	1.720	2.049
Final *R* indices [$I > 2\sigma(I)$]	*R*1 = 0.0515, *wR*2 = 0.1372	*R*1 = 0.0595, *wR*2 = 0.1646
Largest diff. Peak and hole [e Å^{-3}]	2.182 and –1.327	1.012 and –0.755

for emission and excitation, respectively, and a photomultiplier with a photon counting system. The emission spectra were corrected for photomultiplier sensitivity, the excitation spectra for lamp intensity and both for the transmission of the monochromators.

Crystallographic Details: The data collection was performed on a X8 ApexII CCD diffractometer with Mo-K_α radiation (λ = 0.71073 Å). All structures were solved by direct methods and refined by full-matrix least square methods on F^2 with SHELX-97.[60] The plots of the molecular structures were drawn with the Diamond software.[61]

The crystal growth of all products started at 5 °C and continued during one week. No sign of decomposition during storage under nitrogen was observed. Crystallographic data for the structure determinations are listed in Table 4, relevant bond lengths and angles are given in Table 1.

CCDC-748659 (for **9**) and -748560 (for **10**) contain the supplementary crystallographic data for this paper. These data can be obtained free of charge from The Cambridge Crystallographic Data Centre via www.ccdc.cam.ac.uk/data_request/cif.

$[Nd\{OC(C_{14}H_{11}S_2)\}_3(thf)_3]\cdot thf$ (9): To a solution of three equivalents of phenylbis(2-thienyl)methanol (1.009 g, 3.70 mmol) in thf (20 mL) was added one equivalent of $Nd[N(SiMe_3)_2]_3$ (0.771 g, 1.23 mmol) in thf (25 mL). The mixture was stirred at room temperature for two days. The solution was concentrated. Blue crystals were obtained at 5 °C several days later. The isolated yield is 60% (897 mg). ^{1}H NMR (400.13 MHz, $CDCl_3$): δ = 7.3 (br. s, 21 H, 5-H, ϕ-H), 6.9 (br. s, 12 H, 4-H, 3-H), 3.7 (br. s, 8 H, thf), 1.8 (br. s, 8 H, thf), 1.2 (br. s, 12 H, thf), 0.8 (br. s, 4 H, thf) ppm. UV/Vis (190–1100 nm, CH_2Cl_2, 10^{-5} M): λ = 237 nm (ε = 650 × 10^2 M^{-1} cm^{-1}). $C_{61}H_{65}NdO_7S_6$ (1246.73): calcd. C 58.87, H 5.21, Nd 11.56; found C 58.41, H 5.11, Nd 11.00.

$[Nd\{OC(C_{16}H_{13}S)\}_3(thf)_3]\cdot thf$ (10): To a solution of three equivalents of diphenyl(2-thienyl)methanol (0.634 g, 2.38 mmol) in thf (20 mL) was added one equivalent of $Nd[N(SiMe_3)_2]_3$ (0.496 g, 0.79 mmol) in thf (20 mL). The mixture was stirred at room temperature for two days. The solution was concentrated. Blue crystals were obtained at 5 °C several days later. The isolated yield is 34% (328 mg). ^{1}H–NMR (400.13 MHz, $CDCl_3$): δ = 7.3 (br. s, 33 H, 5-H, ϕ-H), 6.9 (br. s, 3 H, 4-H), 6.7 (br. s, 3 H, 3-H), 3.6 (br. s, 5 H, thf), 1.7 (br. s, 6 H, thf), 1.2 (br. s, 10 H, thf), 0.8 (br. s, 12 H, thf) ppm. UV/Vis (190–1100 nm, CH_2Cl_2, 10^{-5} M): λ = 232 nm (ε = 787 × 10^2 M^{-1} cm^{-1}). $C_{67}H_{71}NdO_7S_3$ (1228.66): calcd. C 65.43, H 5.77, Nd 11.73; no satisfactory elemental analysis could be obtained due to the extreme sensitivity of **10**.

Supporting Information (see also the footnote on the first page of this article): Examples of cyclic voltammogram for the compounds **6**–**9**; excitation and emission spectra of **9** and **10**.

Acknowledgments

We gratefully acknowledge the financial support provided by the Deutsche Forschungsgemeinschaft (DFG) in the framework of the SPP1166 (Lanthanoidspezifische Funktionalitäten in Molekül und Material), by the Saarland University and the Fonds der Chemischen Industrie. We thank Dr. Michael Zimmer for the ^{1}H NMR spectra. M. K. and L. G. thank the Centre National de la Recherche Scientifique (CNRS) for financial support.

[1] a) G. E. Buono-Core, H. Li, B. Marcinak, *Coord. Chem. Rev.* **1990**, *99*, 55–87; b) J. Kido, Y. Okamoto, *Chem. Rev.* **2002**, *102*, 2357–2368.

[2] S. Quici, M. Cavazzini, G. Marzanni, G. Accorsi, N. Armaroli, B. Ventura, F. Barigelletti, *Inorg. Chem.* **2005**, *44*, 529–537.

[3] M. P. Oude Wolbers, F. C. J. M. van Veggel, B. H. M. Snellink-Ruel, J. W. Hofstraat, F. A. J. Geurts, D. N. Reinhoudt, *J. Chem. Soc. Perkin Trans. 2* **1998**, 2141–2150.

[4] R. Reisfeld, C. K. Jorgensen, *Laser and Excited states of Rare Earth*s, Springer, Berlin, **1977**.

[5] a) V.-M. Mukkala, M. Helenius, I. K. Hemmilä, J. Kankare, H. Takalo, *Helv. Chim. Acta* **1993**, *76*, 1361–1378; b) G. A. Kumar, R. E. Riman, L. A. Diaz Torrez, O. B. Garcia, S. Banerjee, A. Kornienko, J. Brennan, *Chem. Mater.* **2005**, *17*, 5130–5135; c) G. A. Kumar, R. E. Riman, L. A. Diaz Torrez, S. Banerjee, M. D. Romanelli, T. J. Emge, J. Brennan, *Chem. Mater.* **2007**, *19*, 2937–2946.

[6] a) N. Sabbatini, M. Guardigli, J.-M. Lehn, *Coord. Chem. Rev.* **1993**, *123*, 201–228; b) J. P. Leonard, C. B. Nolan, F. Stomeo, T. Gunnlaugsson, *Top. Curr. Chem.* **2007**, *281*, 1–43.

[7] a) O. Clot, M. O. Wolf, B. O. Patrick, *J. Am. Chem. Soc.* **2001**, *123*, 9963–9973; b) O. Clot, Y. Akahori, C. Moorlag, D. B. Leznoff, M. O. Wolf, B. O. Patrick, M. Ishii, *Inorg. Chem.* **2003**, *42*, 2704–2713; c) V. G. Albano, M. Bandini, C. Moorlag, F. Piccinelli, A. Pietrangelo, S. Tommasi, A. Umani-Ronchi, M. O. Wolf, *Organometallics* **2007**, *26*, 4373–4375.

[8] a) J. Hjelm, R. W. Handel, A. Hagfeldt, E. C. Constable, C. E. Housecroft, R. J. Forster, *Electrochem. Commun.* **2004**, *6*, 193–200; b) J. Hjelm, R. W. Handel, A. Hagfeldt, E. C. Constable, C. E. Housecroft, R. J. Forster, *Inorg. Chem.* **2005**, *44*, 1073–1081.

[9] A.-S. S. Elgazwy, *Appl. Organomet. Chem.* **2007**, *21*, 1041–1053.

[10] M. Beley, D. Delabouglise, G. Houppy, J. Husson, J.-P. Petit, *Inorg. Chim. Acta* **2005**, *358*, 3075–3083.

[11] T. A. Skothiem, R. L. Elsenbaumer, J. R. Reynolds, *Handbook of Conducting Polymers*, 2nd ed., Marcel Dekker: New York, **1998**.

[12] a) X.-Y. Chen, X. Yang, B. J. Holliday, *Polym. Prepr.* **2007**, *48*, 595; b) A. de Bettencourt Dias. Departement of Chemistry, Syracuse University, Syracuse, NY, USA. Abstract of Papers, 232nd ACS National Meeting, San Francisco, CA, United States, Sept. 10–14, **2006**, INOR–102.

[13] D. Wang, D. Cui, W. Miao, S. Li, B. Huang, *Dalton Trans.* **2007**, 4576–4591.

[14] a) J. Lloret, F. Estevan, P. Lahuerta, P. Hirva, J. Pérez-Prieto, M. Sanaù, *Organometallics* **2006**, *25*, 3156–3165; b) S. Destri, M. Pasini, W. Porzio, F. Rizzo, G. Dellepiane, M. Ottonelli, G. Musso, F. Meinardi, L. Veltri, *J. Lumin.* **2007**, *127*, 601–610.

[15] W. S. Hwang, D. L. Wang, M. Y. Chiang, *J. Organomet. Chem.* **2000**, *613*, 231–235.

[16] Y. F. Tzeng, C. Y. Wu, W. S. Hwang, C. H. Hung, *J. Organomet. Chem.* **2003**, *687*, 16–26.

[17] Y.-F. Yuan, T. Cardinaels, K. Lunstroot, K. Van Hecke, L. Van Meervelt, C. Görller-Walrand, K. Binnemans, P. Nockemann, *Inorg. Chem.* **2007**, *46*, 5302–5309.

[18] R. Sultan, K. Gadamsetti, S. Swavey, *Inorg. Chim. Acta* **2006**, *359*, 1233–1238.

[19] a) S. Viswanathan, A. de Bettencourt-Dias, *Inorg. Chem.* **2006**, *45*, 10138–10146; b) A. de Bettencourt-Dias, S. Viswanathan, A. Rollet, *J. Am. Chem. Soc.* **2007**, *129*, 15436–15437.

[20] E. E. S. Teotonio, M. C. F. C. Felinto, H. F. Brito, O. L. Malta, A. C. Trindade, R. Najjar, W. Strek, *Inorg. Chim. Acta* **2004**, *357*, 451–460.

[21] M. Veith, C. Belot, L. Guyard, V. Huch, M. Knorr, M. Zimmer, *Eur. J. Inorg. Chem.* **2008**, 2397–2406.

[22] C. Belot, C. Filiatre, L. Guyard, A. Foissy, M. Knorr, *Electrochem. Commun.* **2005**, *7*, 1439–1444.

[23] R. H. C. Tan, M. Motevalli, I. Abrahams, P. B. Wyatt, W. P. Gillin, *J. Phys. Chem. B* **2006**, *110*, 24476–24479.

[24] F. Quochi, R. Orrù, F. Cordella, A. Mura, G. Bongiovani, *J. Appl. Phys.* **2006**, *99*, 053520.

[25] J.-L. Song, C. Lei, J.-G. Mao, *Inorg. Chem.* **2004**, *43*, 5630–5634.

[26] B. Chen, Y. Yang, F. Zapata, G. Qian, Y. Luo, J. Zhang, E. B. Lobkovsky, *Inorg. Chem.* **2006**, *45*, 8882–8886.

[27] Z. Xie, K. Chui, Q. Yang, T. C. W. Mak, J. Sun, *Organometallics* **1998**, *17*, 3937–3944.

[28] G. R. Giesbrecht, J. C. Gordon, D. L. Clark, B. L. Scott, J. G. Watkin, K. J. Young, *Inorg. Chem.* **2002**, *41*, 6372–6379.

[29] P. B. Hitchcock, M. F. Lappert, I. A. MacKinnon, *J. Chem. Soc., Chem. Commun.* **1988**, 1557–1558.

[30] W. A. Herrmann, R. Anwander, M. Kleine, W. Scherer, *Chem. Ber.* **1992**, *125*, 1971–1979.

[31] J. Gromada, A. Morteux, T. Chenal, J. W. Ziller, F. Leising, J. F. Carpentier, *Chem. Eur. J.* **2002**, *8*, 3773–3788.

[32] L. Guyard, M. Nguyen Dinh An, P. Audebert, *Adv. Mater.* **2001**, *13*, 133–136.

[33] a) X. Wang, G. Shi, Y. Liang, *Electrochem. Commun.* **1999**, *1*, 536–539; b) G. Zotti, A. Berlin, G. Schiavon, S. Zecchin, *Synth. Met.* **1999**, *101*, 622–623; c) S. Abaci, A. Yildiz, *J. Electroanal. Chem.* **2004**, *569*, 161–168; d) K. Palaniappan, J. W. Murphy, N. Khanam, J. Horvath, H. Alshareef, M. Quevedo-Lopez, M. C. Biewer, S. Y. Park, M. J. Kim, B. E. Gnade, M. C. Stefan, *Macromolecules* **2009**, *42*, 3845–3848; e) A. Benedetto, M. Balog, H. Rayah, F. Le Derf, P. Viel, S. Palacin, M. Sallé, *Electrochim. Acta* **2008**, *53*, 3779–3788; f) A. Cithaner, A. M. Önal, *J. Electroanal. Chem.* **2007**, *601*, 68–76; g) A. Arnanz, M.-L. Marcos, S. Delgado, J. Gonález-Velasco, C. Moreno, *J. Organomet. Chem.* **2008**, *693*, 3457–3470.

[34] T. L. Stoot, M. O. Wolf, *Coord. Chem. Rev.* **2003**, *246*, 89–101.

[35] K. R. J. Thomas, J. T. Lin, *Organometallics* **1999**, *18*, 5285–5291.

[36] M. O. Wolf, M. S. Wrighton, *Chem. Mater.* **1994**, *6*, 1526–1533.

[37] W.-Y. Wong, *Comments Inorg. Chem.* **2005**, *26*, 39–74.

[38] L. Guyard, P. Audebert, *Electrochem. Commun.* **2001**, *3*, 164–167.

[39] a) M. Barth, S. Guilerez, G. Bidan, G. Bras, M. Lapkowski, *Electrochim. Acta* **2000**, *45*, 4409–4417; b) L. Guyard, C. Dumas, F. Miomandre, R. Pansu, R. Renault-Méallet, P. Audebert, *New J. Chem.* **2003**, *27*, 1000–1006; c) I. Tabakovic, Y. Kunugi, A. Canavesi, L. L. Miller, *Acta Chem. Scand.* **1998**, *52*, 131–136.

[40] F. Chérioux, L. Guyard, P. Audebert, *Adv. Mater.* **1998**, *10*, 1013–1018.

[41] M. Turbiez, P. Frère, M. Allain, N. Gallego-Planas, J. Roncali, *Macromolecules* **2005**, *38*, 6806–6812.

[42] L. Guyard, F. Chérioux, *Adv. Funct. Mater.* **2001**, *11*, 305–309.

[43] P. Garcia, J.-M. Pernaut, P. Hapiot, V. Wintgens, P. Valat, F. Garnier, D. Delabouglise, *J. Phys. Chem.* **1993**, *97*, 513–516.

[44] P. Bäuerle, U. Segelbacher, A. Maier, M. Mehring, *J. Am. Chem. Soc.* **1993**, *115*, 10217–10223.

[45] P. Hapiot, F. Demanze, A. Yassar, F. Garnier, *J. Phys. Chem.* **1996**, *100*, 8397–8401.

[46] A. F. Diaz, J. Crowley, J. Bargon, G. P. Gardini, J. B. Torrance, *J. Electroanal. Chem.* **1981**, *121*, 355–361.

[47] S. Abaci, A. Yildiz, *J. Electroanal. Chem.* **2004**, *569*, 161–168.

[48] a) P. Audebert, S. Sadki, F. Miomandre, G. Clavier, *Electrochem. Commun.* **2004**, *6*, 144–147; b) W. Zhang, W. Plieth, G. Koßmehl, *Electrochim. Acta* **1997**, *42*, 1653–1661; c) G. Zotti, B. Vercelli, A. Berlin, S. Destri, M. Pasini, V. Hernández, J. T. López Navarrete, *Chem. Mater.* **2008**, *20*, 6847–6856.

[49] R. S. Becker, J. Seixa de Melo, A. L. Maçanita, F. Elisei, *J. Phys. Chem.* **1996**, *100*, 18683–18695.

[50] S. I. Klink, G. A. Hebbing, L. Grave, F. G. A. Peters, F. C. J. M. Van Veggel, D. N. Reinhoudt, J. W. Hofstraat, *Eur. J. Org. Chem.* **2000**, 1923–1931.

[51] A. Dossing, *Eur. J. Inorg. Chem.* **2005**, 1425–1434.

[52] S. Banerjee, G. A. Kumar, R. E. Riman, T. J. Emge, J. G. Brennan, *J. Am. Chem. Soc.* **2007**, *129*, 5926–5931.

[53] J.-C. Bünzli, *J. Alloys Compd.* **2006**, *408–412*, 934–944.

[54] J. Ripoll, L. E. Bausa, C. Terrile, J. G. Sole, F. Diaz, *J. Lumin.* **1997**, *72–74*, 253–254.

[55] Th. Förster, *Discuss. Faraday Soc.* **1959**, *27*, 7–17.

[56] J.-C. Bünzli, *Spectroscopic Properties of Rare Earth in Optical Materials* (Eds.: G. Liu, B. Jacquier), Springer, Berlin, **2005**, chapter 9.
[57] PhD Thesis of Rasa Rapalaviciute, University of the Saarland, Saarbrücken, **2004**.
[58] F. Cherioux, L. Guyard, P. Audebert, *Adv. Mater.* **1998**, *10*, 1013–1018.
[59] B. Abarca, G. Asencio, R. Ballesteros, T. Varea, *J. Org. Chem.* **1991**, *56*, 3224–3229.
[60] G. M. Sheldrich, *SHELX-97*, Program for refinement of crystal structures, University of Göttingen, Germany, **1997**.
[61] *Diamond*, Crystal and Molecular Structure Visualization, CRYSTAL IMPACT, Postfach 1251, 53002 Bonn, Germany (www.crystalimpact.com/diamond/).

Received: October 1, 2009
Published Online: January 12, 2010

